**Rare Metal Materials and Engineering**
Volume 51, Issue 2, February 2022
Available online at www.rmme.ac.cn

Science Press

**Cite this article as**: Li Huaying, Ma Lifeng, Song Yaohui, et al. Effects of Element Cu on Hot Workability of 304L Stainless Steel[J]. Rare Metal Materials and Engineering, 2022, 51(02): 400-407.

ARTICLE

# Effects of Element Cu on Hot Workability of 304L Stainless Steel

**Li Huaying[1], Ma Lifeng[2], Song Yaohui[1], Li Juan[1], Ji Yafeng[2], Liu Haitao[3]**

*[1] School of Materials Science and Engineering, Taiyuan University of Science and Technology, Taiyuan 030024, China; [2] School of Mechanical Engineering, Taiyuan University of Science and Technology, Taiyuan 030024, China; [3] State Key Laboratory of Rolling and Automation, Northeastern University, Shenyang 110819, China*

**Abstract:** The hot deformation behavior of Cu-bearing 304L stainless steel was studied by performing hot compression on Gleeble-3800 thermo mechanical simulator in the temperatures of 900~1150 ℃ and strain rates of 0.01~20 $s^{-1}$, and the processing maps were established by stress-strain curves. Results show that the better processing temperature range is narrowed from 200 °C to 75 °C with the increase of copper content in the alloy (0wt%Cu-304L, 2.42wt%Cu-304L, 3.60wt%Cu-304L). The alloy microstructure characterization reveals that the main causes of instability are local flow instability, shear zone, void and cracking. At the same time, it is found that the plastic deformation can be converted into heat in a short time, leading to the local temperature rise of the deformed materials, which makes the copper segregation area with relatively low melting point easy to form holes and to become the source of cracking, and then reduces the hot workability.

**Key words:** copper-containing antibacterial stainless steel; hot deformation; processing map; instability; microstructure

Antibacterial stainless steels are widely used for artificial joints, food industry, heart stent, etc[1,2]. Compared with light metals, Cu bearing-antibacterial stainless steel is a kind of most frequently applied antibacterial stainless steel, mainly because it has good mechanical properties, excellent exceptional durable performances and manufacturing process[3-6]. Copper precipitation is the key to obtain antimicrobial ability of stainless steel. Some studies[7] on Cu-bearing antibacterial stainless steels showed that nano-scale Cu precipitation have been found by transmission electron microscopy (TEM). Moreover, the addition of Cu can prevent recovery and recrystallization softening, and plays a role of pinning effect by suppressing grain growth because of the formation of $\varepsilon$-Cu phase[8]. Cu precipitation in stainless steels will disturb the passivating oxide layer and intensify the release of Cu ions in biological environments, thereby causing toxicity to the microorganisms. However, relatively higher Cu addition content will lead to "copper embrittlement", which will restrict the industrial production of antibacterial stainless steel during rolling[9]. It is well known that deformation behavior of the steels largely depends on the temperature, strain rate, stress and other environmental factors in hot working[10-14]. Proper Cu content is still controversial for the favorable thermal deformation behavior because the thermal deformation behavior is different for different Cu contents.

Therefore, it is considered to add copper to keep the balance between the antibacterial and hot working properties of Cu-bearing stainless steels. It is of great significance to study the effect of copper content on hot workability. In this work, thermal deformation behavior of austenitic stainless steel containing 0wt%~3.6wt% Cu was studied in the temperature range of 900~1150 °C and strain rate range of 0.01~20 $s^{-1}$ by thermal simulation compression test. By analyzing the deformation microstructure characteristics of the stainless steels in the unstable region, the effect of copper content on hot workability was studied.

Received date: August 26, 2021
Foundation item: Scientific and Technological Innovation Programs of Higher Education Institutions in Shanxi (2020L0333); Natural Science Foundation of Liaoning Province (2019-KF-25-05); Shanxi Province's Key Core Technology and Common Technology Research and Development Project (20201102017); National Key Research and Development Program of China (2016YFB0300205); National Natural Science Foundation of China (52005358)
Corresponding author: Ji Yafeng, Ph. D., Associate Professor, School of Mechanical Engineering, Taiyuan University of Science and Technology, Taiyuan 030024, P. R. China, E-mail: yafengji@tyust.edu.cn

## 1 Experiment

The materials in this study were electroslag remelted stainless steel ingots without copper and with 2.42wt% Cu and 3.60wt% Cu. The chemical compositions are presented in Table 1. The compressed specimens with 10 mm in diameter and 15 mm in height were machined from the ingot. The hot deformation experiments were performed on Gleeble-3800 thermo mechanical simulator. The specimens were heated to 1250 °C at the rate of 10 °C/s, and homogenized at that temperature for 5 min. Subsequently, the specimens were cooled at the rate of 10 °C/s to the desired deformation temperatures of 900~1150 °C (50 °C steps), and then deformed at constant strain rates of 0.01, 0.1, 1, 2.5, 5, 10 and 20 $s^{-1}$ to a target true strain of 0.69. After compression, specimens were immediately quenched using water to freeze the microstructure.

Crystallography investigations were carried out using optical microscopy (OM) and scanning electron microscopy (SEM). The specimens for electron back scatter diffraction (EBSD) analysis were sectioned from the hot deformed samples parallel to the deformation direction. Before OM observation, samples were ground with wet SiC paper up to 2000#, and then mechanically polished with 2.5 and 0.5 μm diamond pastes. Samples were electrolytically etched in a solution of 30% nitric acid for 10 s and washed immediately using alcohol to clearly reveal the austenite microstructure. EBSD tests were performed using a ZEISS field-emission scanning electron microscope. The specimen for EBSD analysis was electrolytically polished using perchloric acid-alcohol solution at 10 V for 30 s at room temperature.

**Table1 Chemical composition of tested steel samples (wt%)**

| Sample | C | Si | Mn | P | S | Cr | Ni | Cu |
|---|---|---|---|---|---|---|---|---|
| 304L | 0.005 | 0.42 | 1.51 | 0.004 | 0.001 | 17.88 | 8.58 | 0 |
| 2.42%Cu-304L | 0.007 | 0.42 | 1.53 | 0.010 | 0.001 | 18.29 | 8.70 | 2.42 |
| 3.60%Cu-304L | 0.007 | 0.49 | 1.54 | 0.013 | 0.001 | 17.91 | 8.72 | 3.60 |

## 2 Results

### 2.1 Microstructure of the as-received coating

The true stress-true strain curves of three steels at strain rates of 0.1 and 10 $s^{-1}$ are shown in Fig. 1. It can be seen that the strain rate increases and the deformation temperature decreases, and the peak stress gradually increases. At the initial stage of deformation, the material is macroscopically dominated by work hardening, the dislocation density increases sharply, and the stress increases sharply. After that, dynamic recovery (DRV) and dynamic recrystallization (DRX) develop rapidly, and the stress increases slowly until it reaches a certain strain, i.e. the stress reaches the maximum. Then it tends to decrease or maintain a stable state, which is the result of dynamic softening at this time. Fig. $1a_1$, $1b_1$, $1c_1$ illustrate that at a low strain rate of 0.1 $s^{-1}$, with the increase of copper content, the temperature of dynamic recrystallization increases from 1100 °C to 1150 °C, which manifests that the rate of recrystallization becomes slow and the softening effect is reduced at the low strain rates. The primary reason for this phenomenon is that the alloys containing copper that is characterized by higher stacking fault energy and small extended dislocation width are prone to pile-up and cross-slip of partial dislocations[15]. In contrast, cross-slip of dislocations is difficult in the alloys with lower stacking fault energy, so DRX will occur when enough dislocations are accumulated in the local area. At the high strain rate of 10 $s^{-1}$, the time for

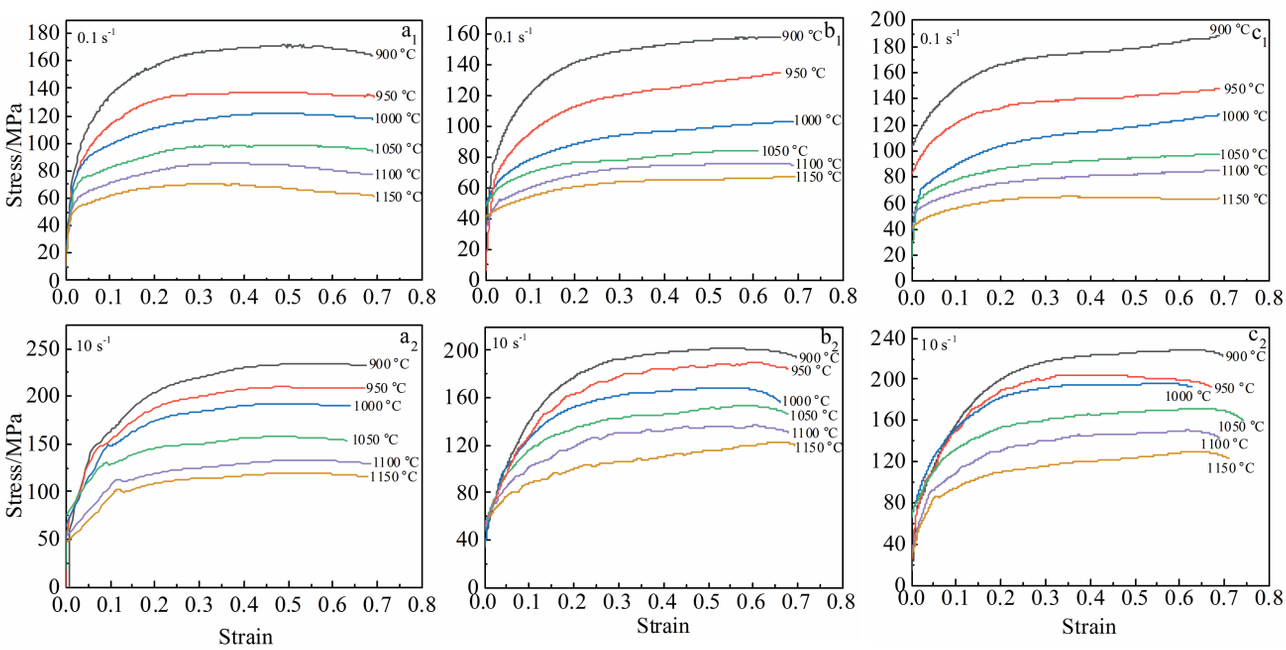


Fig.1 True stress-true strain curves of three kinds of stainless steels under different deformation conditions: ($a_1$, $a_2$) 304L, ($b_1$, $b_2$) 2.42wt%Cu-304L, and ($c_1$, $c_2$) 3.60wt%Cu-304L

DRX is insufficient, leading to a stronger resistance. Therefore, the flow curves at high strain rates are characterized with typical DRV, while those of high temperature and low rates exhibit typical dynamic recrystallization characteristics. In summary, the dominant softening mechanism of copper-containing austenitic stainless steel is DRV followed by DRX.

### 2.2 Processing map

The thermal processing map can reflect microstructure evolution and energy dissipation during thermal deformation. It is helpful to avoid unstable flow regions and to find the optimal hot processing window involving temperature and strain rate[10,16]. Based on the dynamic material model, the $\ln\sigma$-$\ln\dot{\varepsilon}$ curves of thermal simulation compression are fitted by cubic spline interpolation method, and the strain rate sensitivity index $m$ is obtained.

The power dissipation map is usually plotted by power dissipation coefficient $\eta$ (Eq. (1)) in conjunction with deformation temperature and strain rate. A large power dissipation coefficient value is favorable to the occurrence of DRX, which contributes to the structure and performance improvement[17]. Meanwhile, the negative value of ($\dot{\varepsilon}$) can be used as the criterion for judging material instability (Eq. (2)). The instability parameter ($\dot{\varepsilon}$) is related to strain rate and deformation temperature[18]. When the rate of entropy generated in the system is greater than the applied strain rate, local flow instability will occur. In this instability area, defects such as cracking, cavities, local flow, and adiabatic shear bands are prone to occur.

$$\eta = \frac{2m}{m+1} \tag{1}$$

$$\xi(\dot{\varepsilon}) = \frac{\partial \lg\left(\frac{m}{m+1}\right)}{\partial \lg \dot{\varepsilon}} + m \leqslant 0 \tag{2}$$

The power dissipation coefficient $\eta$ and the instability parameter ($\dot{\varepsilon}$) at various strain rates and different temperatures are calculated by Eq.(1) and Eq.(2), respectively. According to the two parameters, the two-dimensional power dissipation contour map combined with the instability map are plotted, and a thermal processing map at the strain of 0.69 is developed. As shown in Fig. 2, the gray shadow zone is the processing instability region, the rest zone is the safety region, and the contour line is the power dissipation coefficient $\eta$. The areas of maximum power dissipation are corresponding to the condition of high temperature and low strain rate. This area is the most favorable to the improvement of the microstructure and properties of Cu-containing antibacterial stainless steel.

The deformation characteristic of 304L stainless steel is similar to 2.42wt%Cu-304L stainless steel. As the temperature increases and the rate decreases, the value of $\eta$ increases diagonally. The power dissipation values of the three steels (304L, 2.42wt%Cu-304L, 3.60wt%Cu-304L) reach the maximum of 58%, 50% and 33%, respectively at 1150 °C/0.01 $s^{-1}$, which is corresponding to process zone I (Fig. 2). The microstructure of this region is prone to DRX. In the region where the rate is higher than 1 $s^{-1}$ and the temperature is above 1050 °C, the value of $\eta$ increases with the increase in temperature and strain rate. The area characterized by power dissipation of ~25% is the process zone II. Compared with the instability zone, it can be seen from Fig. 2 that with the increase of copper content, the instability zone gradually increases and transits to the high temperature zone, the machinable zone shrinks to the high temperature zone, the processing temperature range shrinks from 200 °C to 75 °C, and the hot processing window becomes narrower, as shown in Table 2.

### 2.3 Microstructure evolution

According to the thermal processing map at the strain of 0.69 and the deformation microstructure of different regions, the deformation mechanism of hot processing region is identified. Fig. 3 shows the microstructures of 2.42wt% Cu-304L, 304L and 3.60wt% Cu-304L obtained by EBSD. The black lines are large angle grain boundaries (>15°), the red lines are sub-grain boundaries (2°~15°), and the yellow lines are twin boundaries. The blue phase is ferrite, and the dark one is austenite. Fig.3a shows the microstructure of the 2.42wt%Cu-304L steel in the hot-processing zone I at 1150 °C/0.01 $s^{-1}$. It is distinct that austenite is uniform and equiaxial due to the complete DRX under the condition of high temperature and low strain rate. Correspondingly, the power dissipation coefficient $\eta$ of this zone is about 50%, which is a relatively easy processing area. Fig.3b shows the microstructure of 304L steel at 1150 °C/10 $s^{-1}$. Higher temperature and larger strain rate increase the heat energy and make the structure reach

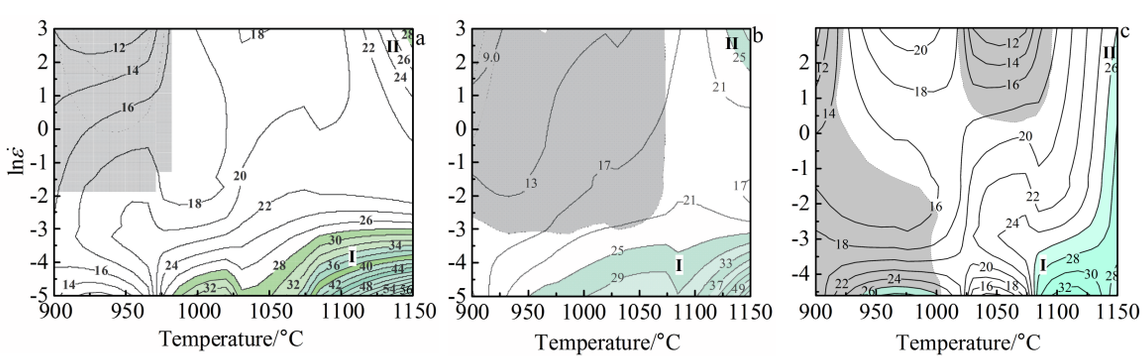


Fig.2 Hot processing maps of three kinds Cu-bearing austenitic steel: (a) 304L, (b) 2.42wt%Cu-304L, and (c) 3.60wt%Cu-304L

**Table 2 Processing window of three kinds of Cu-bearing austenitic steel samples**

| Sample | Temperature/°C | Strain rate/$s^{-1}$ |
|---|---|---|
| 304L | 1000~1150 | 0.01~0.1 |
| 2.42%Cu-304L | 1050~1150 | 0.01~0.1 |
| 3.60%Cu-304L | 1075~1150 | 0.01~0.05 |

a stable flow state. At the same time, it is found that small grains appear around the large grains in the structure, indicating that DRX occurs. Because of the high strain rate, some small equiaxial grains are generated at the original grain boundaries. Combined with the stress-strain curves, the microstructure undergoes DRV and partial DRX. Fig. 3b~3d also show that the blue ferrite is distributed in the matrix in sheets. When added copper content is 2.42wt%, the ferrite is reduced, and the deformed austenite grains contain twins (Fig. 3c). For 3.60wt% Cu-304L steel (Fig. 3d), ferrite is dispersed along the grain boundaries, and the newly formed recrystallized grains are distributed around the large grains. Moreover, the majority of austenite grains contain twins, and the amount of ferrite decreases.

The instability phenomenon during plastic deformation mainly includes local plastic flow, adiabatic shear band, cavity and cracking. Fig.4 shows the microstructures of the gray area in the hot processing diagram. As marked by the arrows in Fig. 4a, the slip bands are closely aligned in the 304L steel under the condition of 900 °C/20 $s^{-1}$, which causes local flow instability. Moreover, continuous shear bands are formed at the high strain rates. In 2.42wt%Cu-304L steel, fine recrystallized grains are developed around the shear bands. In addition, a large number of cavities with a size of ~20 μm are observed in the grain boundaries and phase boundaries. Fig. 4c shows the microstructure of 3.60wt% Cu-304L steel at low temperature and high strain rate. The local microstructure is severely distorted, resulting in less heat transfer and accelerated deformation, with consequent formation of adiabatic shear bands. The crack is developed on an angle of 45° to the shear bands. A large number of cracks can also be seen in Fig.4c, which may be caused by holes in the structure. Meanwhile, recrystallized grains are observed around the cracks. These fine recrystallizations deform the favorable crystal orientation. At the same time, the adjacent grains are restrained, the continuation of the crack is prevented, and the power dissipation factor is reduced to 9%. In summary, it can be seen from the instability phenomenon that with the increase of copper content, the main change law is local flow instability, shear zone+void, and shear zone+cracking.

## 3 Discussion

Based on the above experimental results, it can be seen that the hot workability of the experimental steels decreases with the increase of copper content, and the range of processing temperature is narrowed. As shown in Fig. 4, when 2.42wt%Cu-304L steel and 3.60wt% Cu-304L steel were subjected under the deformation condition of 900 ° C/20 $s^{-1}$, large plastic distortion occurs locally, and the adiabatic shear bands are developed. It is generally believed that the addition of copper can improve the stacking fault energy of the alloy and change the deformation mechanisms[19,20]. With the increase of stacking fault energy, the deformation mechanism can change from dislocation slip to plane slip, twin deformation and

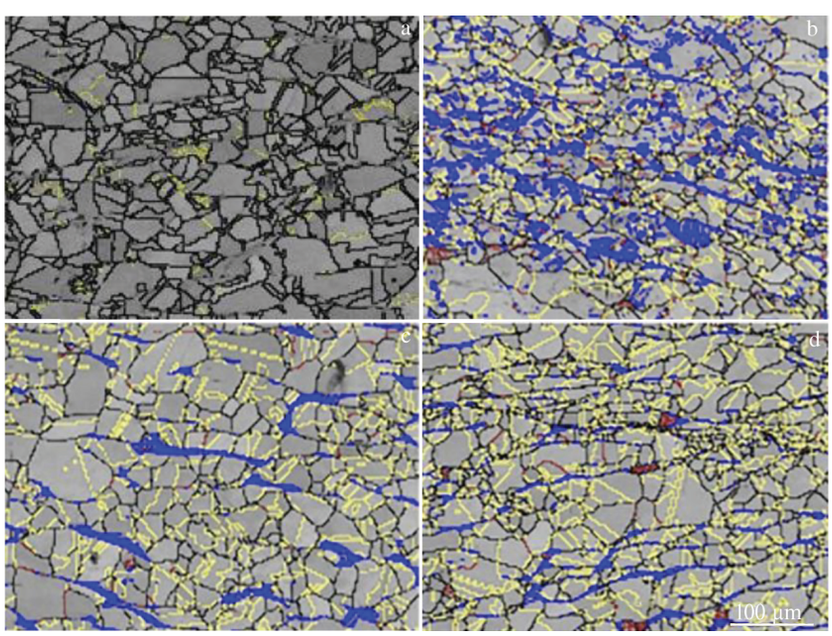


Fig.3 Grain boundary diagrams of copper-bearing steels processed in zones I and II: (a) 2.42wt%Cu-304L steel at 1150 °C/0.01$s^{-1}$, (b) 304L steel at 1150 °C/10 $s^{-1}$, (c) 2.42wt%Cu-304L steel at 1150 °C/10 $s^{-1}$, (d) 3.60wt%Cu-304L steel at 1150 °C/10 $s^{-1}$ (the blue is ferrite, the black is >15° high angle grain boundary, the red is 2°~15° sub-grain boundary and the yellow is twin grain boundary)

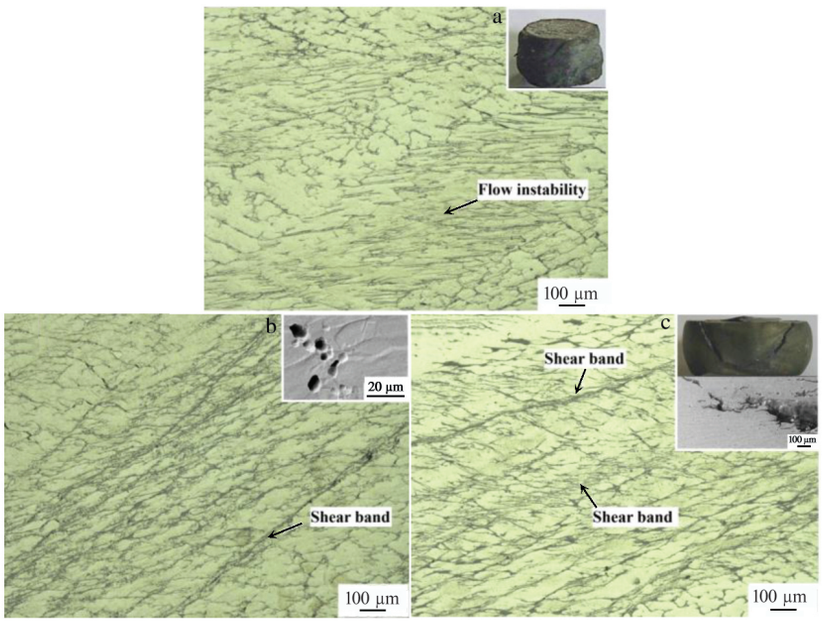


Fig.4 Corresponding microstructures of three copper-containing steels in the unstable zone: (a) 304L at 900 °C/20 $s^{-1}$, (b) 2.42%Cu-304L at 900 °C/20 $s^{-1}$, and (c) 3.60%Cu-304L at 900 °C/20 $s^{-1}$

finally the trend of micro band, and twin deformation can improve the plasticity and processing properties of the metal.

However, according to the experimental results, the plasticity is deteriorated with the increase of copper content. The deformation process involves local flow instability, shear band, cracking, etc. Thus, the plastic instability is intensified. In order to find out the underlying reasons for the unusual phenomenon, the microstructure was observed by TEM. As shown in Fig. 5, there are a large number of tiny ellipsoidal precipitates (about 0.8 μm) in the two experimental steels.

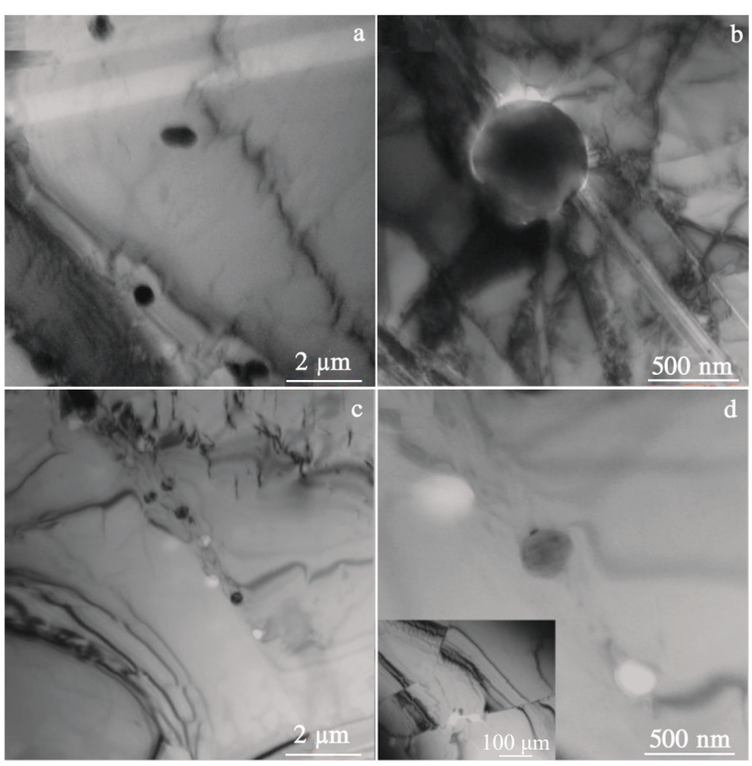


Fig.5 TEM images of two steels deformed under 1050 °C/2.5 $s^{-1}$: (a, b) 2.42wt%Cu-304L steel and (c, d) 3.60wt%Cu-304L steel

Because precipitations hinder the dislocation motion and the migration of the sub-grain boundaries, DRX and DRV are inhibited [21,22], leading to degradation of plasticity and hot workability. Moreover, the inhibition of deformation twins also aggravates the non-uniform deformation, resulting in local flow instability, shear band and cracking. As evidenced in Fig. 5b, the twins are blocked by a spherical precipitate, which indicates that the precipitation of copper element hinders the development of twins. It is generally acknowledged that the deformation twins promote the plastic deformation by adjusting the orientation relationship, which is beneficial for improving the deformation uniformity. Because the deformation twins are suppressed, the uniformity of plastic deformation is destroyed, leading to the aggravation of deformation instability.

When the copper content increases to 3.60wt%, under the same thermal deformation conditions, as shown in Fig. 5c, the amount of spherical precipitates increases which are dispersed around the grain boundaries. Therefore, the increase of copper content causes a large amount of copper-rich precipitates around the grain boundaries. Moreover, the size of the precipitates decreases with increase in copper content, and it is estimated to be about 0.3 μm. At a higher strain rate, the internal temperature of the material rises instantly, and part of the copper-rich phase begins to become liquid. These copper-rich phases precipitated around the grain boundary will penetrate into the grain boundary and cause cracking. Therefore, the increase in copper content increases the copper-rich phase, which becomes a potential condition for thermal deformation and cracking of the material, and in turn promotes the instability of the phenomenon.

When the temperature exceeds the melting point temperature of copper (1083.4±0.2 °C), as shown in Fig. 6, the size and quantity of precipitates decrease with the increase of copper content under 1100 °C/2.5 $s^{-1}$ deformation condition. In Fig. 6, the precipitated phases in the 2.42wt% Cu-304L steel are spherical with a size of 0.29 μm; the precipitated phases in the 3.60wt%Cu-304L steel are dots with a size of 0.03 μm that are scattered in the matrix. Different from carbides and nitrides, the size of the copper-rich precipitation phase in steel is usually very small, and it is not easy to directly characterize. In the process of high temperature and high rate deformation, a large number of dislocation entanglements appear in the crystal. The larger the deformation, the higher the dislocation density, which provides a favorable position for the copper diffusion phase.

In addition, as shown in Fig. 7, as-cast ferrite characterized by pentagonal star is found in 3.60wt%Cu-304L steel. Because of the high alloying element content in the 304L stainless steel, the dendritic segregation is severe, and the columnar crystals are coarser. Generally, some high-temperature $\delta$ ferrites are retained during solidification in austenitic stainless steel. Although retained ferrite is generally considered to be effective in improving stress corrosion resistance and intergranular corrosion resistance in steel[14,23], it also significantly reduces the ductility and workability of steel.

The composition of ferrite was analyzed by EDS. It is obvious that Cr is abundant in ferrite, while the content of Ni in the surrounding austenite matrix is higher. From the line scan, a peak of copper element around the phase boundary is observed, indicating that copper element is segregated at the phase boundary. At the higher strain rates, the local energy is difficult to be released, so the softening effect and the value of $\eta$ are reduced, leading to stress concentration in local large

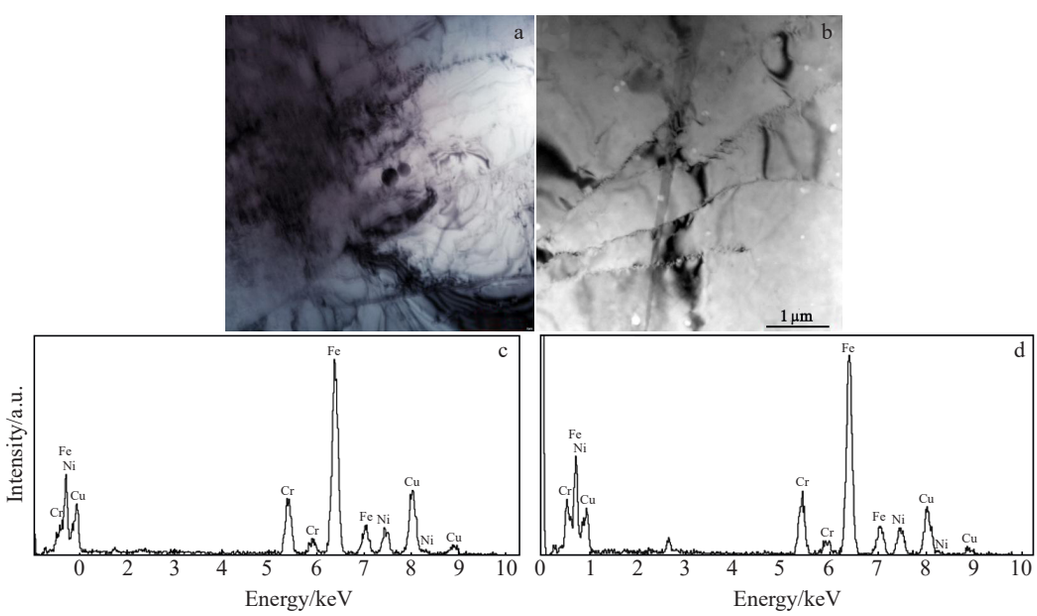


Fig.6 TEM images (a, b) and EDS spectra (c, d) of two steels deformed under 1100 °C/2.5 $s^{-1}$: (a, c) 2.42wt%Cu-304Lsteel and (b, d) 3.60wt%Cu-304L steel

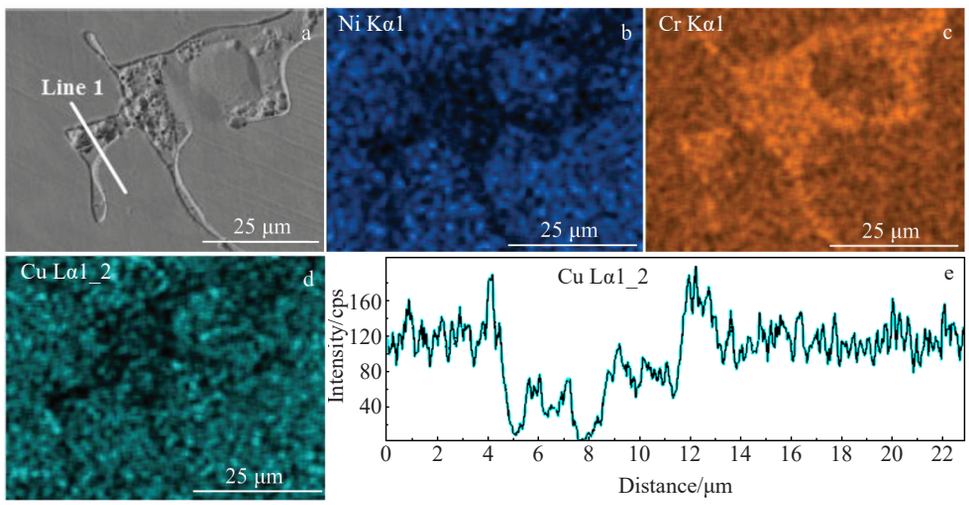


Fig.7 SEM image (a), EDS element mappings of Ni (b), Cr (c), Cu (d) for as-cast 3.60wt%Cu-304L steel, and EDS line scan results of Cu along line 1 marked in Fig.1a (e)

deformation regions. Moreover, the local plastic deformation can be converted into heat in a short time, resulting in the rise of temperature of the deformed zone. Therefore, the copper segregation region with relatively low melting point is easy to form pores, which become the source of cracking (as evidenced in Fig. 4). Meanwhile, the hot workability is reduced.

## 4 Conclusions

1) Comparing the processing range of antibacterial austenitic stainless steel with different copper contents, it is found that as the copper content increases, the processing temperature range is shrunk from 200 °C to 75 °C, and the hot processing window is narrowed.

2) As the copper content increases, the ferrite content in the tested steel gradually decreases. In the instability zone corresponding to the processing drawing (900 °C/20 $s^{-1}$), as the copper element increases, the main causes of instability in the structure are local flow instability, shear zone+cavity, and cavity+shear zone+cracking .

3) The spherical precipitates hinder the development of twinning, which will destroy the uniformity of plastic deformation and aggravate the instability of deformation. In addition, plastic deformation will cause the temperature rise in a short time. Under the influence of stress concentration, the melting point is low, and the copper-rich phase is easy to be melted to form voids, which will become the source of cracks, and then reduce the hot workability of the material.

## References

1 Ma Tao, Li Yungang. *Surface Technology*[J], 2016, 45: 134

2 Wang Qiang, Ren Ling, Li Xiaopeng *et al*. *Materials Science & Engineering C*[J], 2016, 68: 519

3 Zhao Zhanyong, Bai Peikang, Misra R D K *et al*. *Journal of Alloys and Compounds*[J], 2019, 792: 203

4 Zhao Shuming, Li Jing, Bai Peikang *et al*. *Metals*[J], 2019, 9: 267

5 Zhao Zhanyong, Bai Peikang, Li Liang *et al*. *Materials*[J], 2019, 12: 330

6 Hong I T, Koo C H. *Materials Science and Engineering A*[J], 2005, 393: 213

7 Li Hengwu, Zhang Tibao, Zhang Tiyun *et al*. *Acta Metallurgica Sinica*[J], 2008, 44(1): 39 (in Chinese)

8 Soylu B, Honeycombe R. *Materials Science and Technology*[J], 2013, 7: 137

9 Li Xincheng, Liu Jie, Zhu Weixing *et al*. *Advanced Materials Research*[J], 2014, 3593: 27

10 Huang H Q, Di H S, Yan N *et al*. *Acta Metallurgica Sinica*[J], 2018, 31: 503

11 Mataya M C, Nilsson E R, Brown E L *et al*. *Metallurgical and Materials Transactions A*[J], 2003, 34: 1683

12 Qin Fengming, Zhu Hua, Wang Zhenxing *et al*. *Materials Science and Engineering A*[J], 2017, 684: 634

13 Yang K, Dong J, Chen S *et al*. *Chinese Journal of Materials Research*[J], 2006, 20: 523

14 Song Yaohui, Li Yugui, Zhao Guanghui *et al*. *Steel Research International*[J], 2021, 92: 2 000 587

15 Tong Xi, Babar Shahzad M, Xu Dake *et al*. *Materials Science and Engineering C*[J], 2017, 71: 1079

16 Khorshidi H, Kermanpur A, Rastegari H *et al*. *Materials Today Communications*[J], 2021, 27: 102 352

17 Dipti Samantaray, Sumantra Mandal, Vinod Kumar *et al*. *Materials Science and Engineering A*[J], 2012, 552: 236

18 Prasad Y. *Indian Journal of Technology*[J], 1990, 28: 435

19 Dumay A, Chateau J P, Allain S *et al*. *Materials Science and Engineering A*[J], 2006, 483: 184

20 Choi Jeom Yong, Jin Won. *Scripta Materialia*[J], 1997, 36: 99
21 Song Hyejin, Yoo Jisung, Kim Sang Heon *et al*. *Acta Materialia* [J], 2017, 135: 215
22 Zhou G, He X. *WISCO Technology*[J], 2003, 3, 24
23 Emami S, Saeid T, Khosroshahi R A. *Journal of Alloys & Compounds* [J], 2017, 739: 678

# 铜元素对304L不锈钢热加工性能的影响

李华英[1]，马立峰[2]，宋耀辉[1]，李　娟[1]，姬亚锋[2]，刘海涛[3]
(1. 太原科技大学 材料科学与工程学院，山西 太原 030024)
(2. 太原科技大学 机械工程学院，山西 太原 030024)
(3. 东北大学 轧制技术及连轧自动化国家重点实验室，辽宁 沈阳 110819)

**摘　要：**采用Gleeble-3800热模拟试验机对含铜304L不锈钢进行热压缩实验，变形温度为900~1150 ℃，应变速率为0.01~20 $s^{-1}$，并通过应力-应变曲线构建其热加工图。结果表明，随着铜含量的增加（0%Cu-304L，2.42%Cu-304L，3.60%Cu-304L），较好的热加工温度范围从200 ℃降低到75 ℃。微观组织分析发现：该材料失稳的主要原因有局部流动失稳、剪切带、空洞和裂纹；在热变形过程中，塑性变形能在短时间内转化为热量，导致变形材料局部温度升高，这使得熔点相对较低的铜偏析区易融化从而形成孔洞，成为裂纹的来源，降低了材料的热加工性。

**关键词：**含铜抗菌不锈钢；热变形；热加工图；失稳；微观组织

作者简介：李华英，男，博士，副教授，太原科技大学材料科学与工程学院，山西 太原 030024，E-mail：2014246@tyust. edu. cn